Colour and multispectral imaging for wound healing evaluation in the context of a comparative preclinical study

Dorra Nouri, Yves Lucas, Sylvie Treuillet, Romuald Jolivot, Franck Marzani

Colour and multispectral imaging for wound healing evaluation in the context of a comparative preclinical study

Dorra Nouri*[a], Yves Lucas[a], Sylvie Treuillet[b], R. Jolivot[c], F. Marzani[c]
[a]Laboratoire PRISME, IUT Bourges, Université d'Orléans, 63 avenue de Lattre de Tassigny, 18020 Bourges cedex, France
[b]Laboratoire PRISME, Polytech' Orléans, Université d'Orléans, 12 rue de Blois BP 6744, 45067, Orléans cedex 2, France
[c]LE2i UFR Sciences et Techniques, Université de Bourgogne, allée Alain Savary, 21000 Dijon, France

ABSTRACT

Accurate wound assessment is a critical task for patient care and health cost reduction at hospital but even still worse in the context of clinical studies in laboratory. This task, completely devoted to nurses, still relies on manual and tedious practices. Wound shape is measured with rules, tracing papers or rarely with alginate castings and serum injection. The wound tissues proportion is also estimated by a qualitative visual assessment based on the red-yellow-black code. Further to our preceding works on wound 3D complete assessment using a simple freehanded digital camera, we explore here the adaptation of this tool to wounds artificially created for experimentation purposes. It results that tissue uniformity and flatness leads to a simplified approach but requires multispectral imaging for enhanced wound delineation. We demonstrate that, in this context, a simple active contour method can successfully replace more complex tools such as SVM supervised classification, as no training step is required and that one shot is enough to deal with perspective projection errors. Moreover, involving all the spectral response of the tissue and not only RGB components provides a higher discrimination for separating healed epithelial tissue from granulation tissue. This research work is part of a comparative preclinical study on healing wounds. It aims to compare the efficiency of specific medical honeys with classical pharmaceuticals for wound care. Results revealed that medical honey competes with more expensive pharmaceuticals.

Keywords: wound assessment, SVM classification, active contour, KNN classification, multispectral imaging.

1. INTRODUCTION

The quantitative assessment of chronic wounds is generally based on two types of clinical review: a visual review for wound tissue identification from dominant colors and a manual review for wound measurements check to describe the wound shape (area, perimeter, depth, etc.). Currently, there are two techniques for these examinations: (1) the direct manual method used by clinicians to measure periodically the wound dimensions using a millimeter ruler. This technique is simple, but the calculation of dimensions of the wound is inaccurate. (2) Another method is to copy the wound boundaries on transparent tracing paper placed on a metric grid. The wound surface is then determined by counting the number of squares manually or automatically after scanning the image. However, the step of counting the squares is tedious and the transparent tracing paper can lead to infection problems. Methods based on image processing have been proposed as alternative techniques for wounds assessment because they provide objective, reliable and reproducible measures. In addition, infection problems are not posed as there is no contact between the wound and the measurement system.

By the 90s, many works have been performed for analyzing and monitoring the wounds evolution. The main differences between these studies related on wound types (pressure sores, lesions, ulcers, etc.) and the objective. For some, it is to extract an overall indication of healing to measure the wound surface[1, 2] or the amount of fibrin in the ulcer area with a semi-automatic method based on adaptive spline technique in the HSV space[3]. Other works focused on the relation between the wounds color and the presence of inflammation[4] and on the identification of all the wound tissues[5].

*dorra.nouri@univ-orleans.fr; phone (0033) 248238218

In our previous work on ulcers and bedsores, we developed an innovative tool for chronic wounds assessment with a simple digital camera for colorimetric analysis and dimensional tissue measurement[6, 7]. Those previous works were carried out on RGB images.

The multispectral imaging is another technique used for wound assessment. The basic idea of this technique is to acquire a series of images at different wavelengths. Currently, multispectral imaging is applied in several medical fields such as histology[8, 9] and dermatology for the detection and diagnosis of lesions on the skin[10, 11, 12]. In order to assess developing foot ulcers for diabetic patients, an in vivo map for skin chromophores was carried out[13, 14]. A multispectral camera is also used to quantify metabolic parameters of the oxygen saturation of the skin as a way to describe in detail the condition of a wound[15].

In this paper, we study the wound assessment in the context of a preclinical study in apitherapy. The main objective is to process two types of imaging: RGB images acquired by a simple digital camera and multispectral images acquired by a multispectral camera. For color images, we applied two imaging techniques: the unsupervised active contour method and the supervised support vector machine (SVM) classification method. For multispectral images processing, we applied the same active contour method and we compared it to the k-nearest neighbor classification method. The outline of the paper is as follows. In the next section we describe the different processing applied to the RGB and multispectral imaging. Experimental results and comparison of both methods are presented in the second section. Finally, wound surfaces are compared to assess the wound healing rate.

2. METHODOLOGY AND MATERIAL

2.1 Color images processing

2.1.1. Preprocessing steps

Before the following processing, an intermediate preprocessing steps were applied in which manual labeling, color and scale correction were carried out. In the first step, the wound database images were labeled by medical experts through a graphical interface to create a ground truth useful for the supervised method (Fig.1). This manual labeling was applied on the images after an unsupervised segmentation using JSEG algorithm[16]. In the next step, standard color correction was applied using the Retinex white patch method[17] followed by polynomial correction of color sRGB components[18]. The color correction was performed to overcome the lighting variations, the reflectivity of the skin tissue and the position of the shots which affect the tissue colors in the image and consequently the obtained quantitative measures. We designed a contextual 24 patches color pattern placed in the field of view, composed only of representative color samples extracted from a wound database (Fig.1). The contextual color chart was also used in the third preprocessing step to correct and to calculate the scale factor from which the wound surfaces were determined in real dimensions (cm²). To overcome the misalignment of the chart with the camera optical axis because of the curved back of the animal, we applied the analytical method[19] to calculate the orientation of the camera in the coordinate of the color chart.

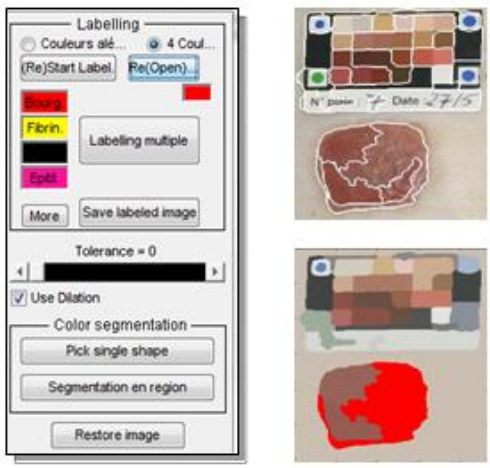

Figure 1. Labeling interface for the ground truth construction. Pre-segmented images are used to help medical expert coloring each region in the wound.

2.1.2. Active contour method

The basic idea of active contour models is to evolve a curve so as to minimize a given energy functional in order to produce the desired segmentation and detect objects in the image. Two main categories exist for active contours models: edge-based and region-based. The first approach, also called *snakes*, is based on the image gradient to stop the contour evolution in order to identify object boundaries[20, 21]. One benefit of this type of flow is the fact that no global constraints are placed on the image. However, this method is very sensitive to image noise and highly dependent on initial curve placement[22]. The second approach is based on Mumford–Shah segmentation techniques for stopping term[23] and on the level set method for curve evolution[24]. The main advantages in this method compared to edge-based method are robustness against initial curve placement and insensitivity to image noise. In fact, interior contours are automatically detected starting with only one initial curve. The position of the initial curve can be anywhere in the image, and it does not necessarily surround the objects to be detected. For our study our main goal through applying the active contour method is to detect the homogenous region in the images that represents the wound differently from the healthy skin. Thus, we chose region-based approach and especially the classical and founder model proposed by Chan and Vese[25] and whose implementation is available[26]. To improve the segmentation results, we performed a pixel filling step and the wound surfaces using the scale factor previously mentioned were computed.

2.1.3. SVM classification

The wounds evolution was also studied by applying tissue classification process which was preceded by an unsupervised step of segmentation using JSEG algorithm[16]. The basic idea of this algorithm was to divide the segmentation process in two steps: color quantization and spatial segmentation. The first step aimed to limit the number of colors in the image by quantification to a few dominant tones preserving a good natural representation of images. The second step, performed on the quantized image, consisted in the spatial segmentation using a homogeneity criterion *J* which was calculated in a neighborhood around each pixel restricted to generate a *J-image* where a *J* value was assigned to each pixel. The lowest values were at the homogeneous regions centers, while the highest ones drew region boundaries. A method of region growing applied to the *J-image* provided segmentation of the original image.

The tissue classification process was divided into three main stages: the first one is the regions characterization followed by the extracted data packaging step and finally the tissue labeling. The classification process begins with the regions characterization by computing colour (mean components, histograms, dominant colours) and texture (co-occurrence matrix "GLCM", Gabor filters, local binary patterns) descriptors. Then a reconditioning step is applied using principal component analysis to avoid redundancy and to reduce dimensionality[6]. In the third step, different vectors are separated and the regions class belonging to each tissue type is identified. The classifier used in this stage is a supervised one based on a support vector machine. The ground truth obtained from the labeled half of the images database was used as training set for the SVM classifier configured with a perceptron kernel[7]. Its robustness was evaluated using the second unlabeled half of the image database.

2.2 Multispectral images processing

2.2.1. Multispectral imaging system

The second part of this preclinical study is the evaluation of wound healing by processing multispectral images. They were acquired by a multispectral system that covers the visible and the near infrared range of the spectrum [430 nm – 780 nm]. This system, called ASCLEPIOS (Analysis of Skin Characteristics by Light Transmission and Processing Image Of Spectrum), was developed and validated for dermatological applications in the Le2i laboratory in Dijon[27]. The system is coupled with software that reconstructs the reflectance cube (hyperspectral cube) from the acquired filtered images. ASCLEPIOS is decomposed in two parts: a light source compartment and a hand-held acquisition device. The illumination compartment houses the light source (Sutter Instrument, model Lambda LS Xenon Arc), and the spectral selective device. The latter is based on ten medium bandpass interference filters (CVI Melles Griot) which are held on a filter wheel (Sutter Instrument Lambda 10-3, model LB10-NW) yielding a switching times of 40 milliseconds between adjacent filters. The acquisition system is based on a monochromatic CMOS digital sensor (Photonfocus Model MV1-D1312l-160-CL) that provides a spatial resolution of 32 pixels.mm^{-1} and producing an acquisition region of size 32 x 38 mm with a depth of 5 mm. The camera offers a 1.4 Megapixels resolution (1312 x 1082 pixels) and it is integrated into a handheld device to ensure an ergonomic acquisition images. The control of the filter wheel, the data acquisition and the generation of reflectance cube are performed using appropriate software installed on the computer (Figure 2).

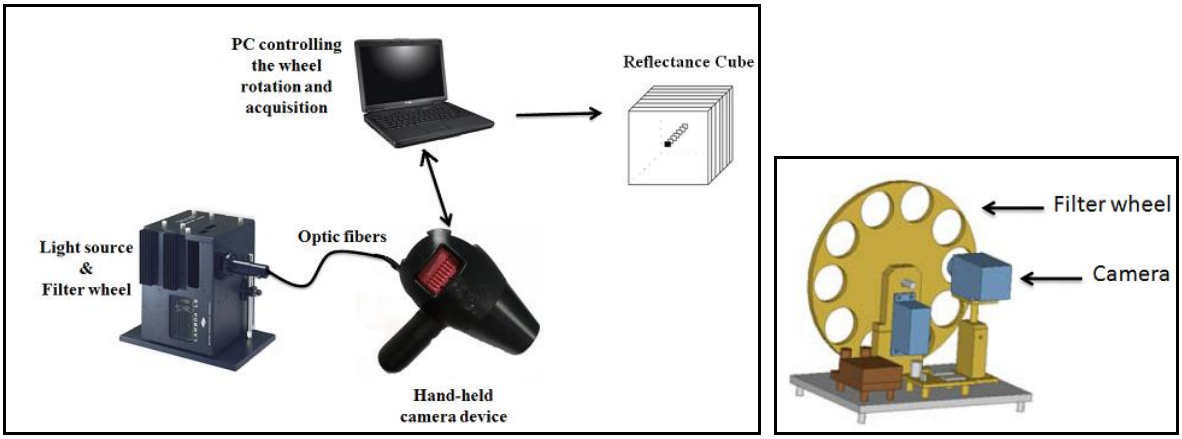

Figure 2. ASCLEPIOS multispectral imaging system overview (left). The spectral selective device (right).

2.2.2. Spectral signature

From the collected multispectral images, hyperspectral (HS) cube was generated to provide rich spectral data which may reveal certain spectral properties or attributes not initially obvious in multispectral images. The reconstructed reflectance cube represents a 3-dimensional volume (x, y, λ) where x and y are for spatial dimensions and λ is for spectral dimension (Fig. 3 left). In our case, a neural network expanded the spectral resolution to reconstruct a 36 wavelength reflectance HS cube[28]. The HS cube increased the spectral resolution without increasing the number of filters and important information can be extracted through the reflectance spectrum that characterizes each pixel. The Fig.3 right illustrates the spectral signatures of three regions in the multispectral images: the healthy skin, the granulation (the red region in the wound) and the epithelium that marks the end of the wound healing. Each mean reflectance spectrum was computed in a 20 x 20 pixels window for the three regions in the spectral range of [430 nm – 780 nm].

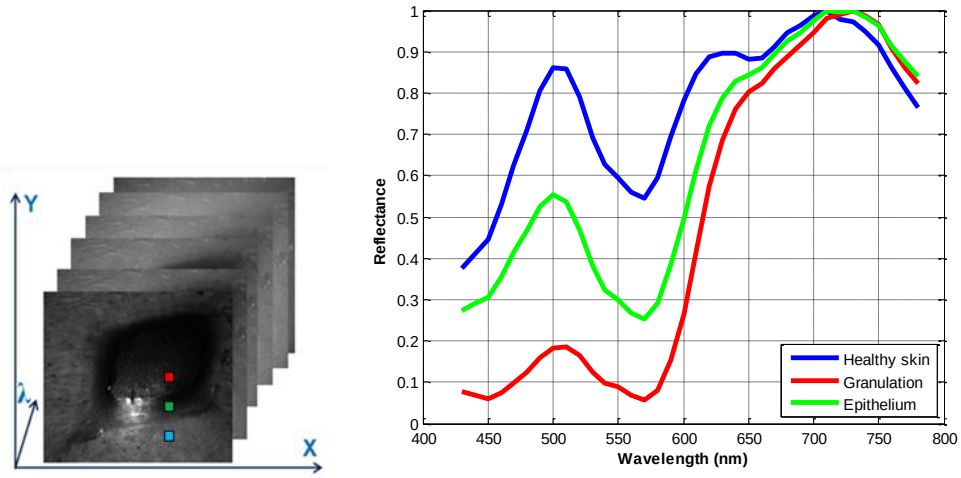

Figure 3. The hyperspectral cube with three dimensions (x, y, λ) (left). The reflectance signatures of each type of wound tissue: blue: healthy skin, red: granulation and green: epithelium (right).

2.2.3. Active contour method

In this section we had applied the same unsupervised method of region-based active contour previously used for color images. Detailed information about the basic idea of the algorithm and its implementation are mentioned in the section 2.1.2. The active contour was applied in multispectral images at 500 nm where the spectra showed great disparities and the contrast between each wound tissues must be distinguished (Figure 3 right). Then, the wound surfaces were determined.

2.2.4. KNN classification

The classification approach adopted in this study is a simple supervised classification algorithm using the K-Nearest Neighbors[29] (KNN).The basic idea of this method is predicting the class of a test example. In fact, it aims to find the k training samples to determine the k-nearest neighbors based on a distance measure. Next, the majority of the k nearest neighbors decides the class of the next instance. Thus, the method uses two parameters: the number *k* and the similarity function or metric to compare the new case to those already classified. The parameter $k \in N$ is chosen depending on the given data set dimensions. To avoid equal votes in binary classification, the best choice is to take a *k* odd value. For high dimension learning databases, a high *k* value reduces the noise effect on the classification and hence the problem of over-learning. However, it may fall into the over-smoothing problem where the boundaries between classes are not distinct. Several heuristics techniques aim to select the value of *k* such as the cross-validation method[30, 31], which find the best value of k minimizing the classification error. The most commonly used and simplest metric used for KNN algorithm is the Euclidean distance especially in the case where each observation is a fixed length vector consisted of real numbers. In our case, a database composed of six vectors characterizing the three different regions of the image (healthy skin, granulation and epithelium) was constructed. Each tissue type was assigned to a class formed by two vectors that included the 36 descriptors corresponding to the mean reflectance values in a 40x40 pixels window over the HS cube images. Hence, we chose k=1 as we have a small learning dataset and we want a good distinction between the three classes boundaries so that we can separate the three tissue types in the wound images.

3. RESULTS

3.1 Preclinical study protocol

The preclinical study was conducted in the context of apitherapy which refers to medical care based on honeys. This study aimed to compare the efficiency of medical honeys with classical pharmaceuticals. The clinical protocol consisted in making two series of artificial eight wounds (3 x 3 cm^2) on a pig's back to be treated, one half with commercial products (Gelonet, Alginate, Aquacell Argent, Melifarm), and one half with medical thyme honey. A colour digital camera (Canon EOS 350D) with annular flash was used to acquire wound images (2304x3456 pixels) every three days during two weeks. Multispectral images were acquired using ASCLEPIOS system every week (Cf. Section 2.2.1).

3.2 Experimental results of RGB images

Fig. 4 shows the result of the active contour based-region method applied to wound RGB images. A filling region step was carried out to enhance the homogeneous region of the wound on the binary image. Then the wound surfaces were calculated in cm^2 after correcting the scale factor. These results were compared to the results of wound surfaces calculated in the manual labeled wound images. The graph illustrated in Fig. 4 represents the linear regression plot and shows a correlation index $R^2 = 0.9947$. Fig. 5 shows the results of SVM classification applied on the test database composed by the half initial dataset. As wounds are neither infected nor necrotic, we have a single wound tissue class. The wound surfaces were calculated from the number of pixels retained by the mask over the image. These results were compared with those obtained by the method of the active contour. Both approaches were applied to the same wounds after removing a few outliers rejected by the classification. Figure 6 shows that the active contour method is more robust for the RGB images as it presents the highest correlation index.

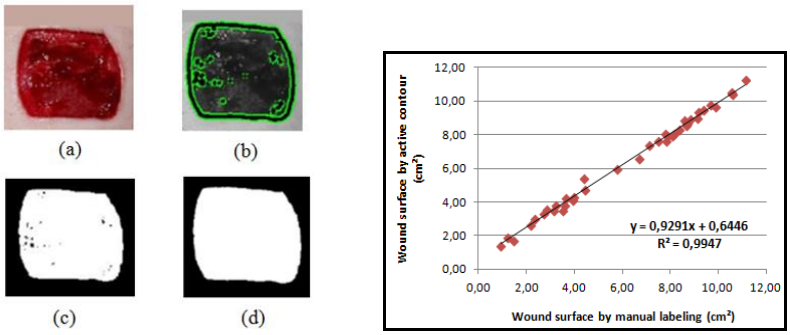

Figure 4. (left) Active contour method applied on RGB image: original wound image (a), active contour image (b), binary image mask (c) and result after region filling step (d). (right) Linear regression plot between results obtained by the active contour method and the manual labeling.

(a) (b) (c)

Figure 5. Results of the SVM classification. (a) original wound image (b) wound region automatically detected by the SVM classifier. (c) mask applied to detect the "wound" class pixels.

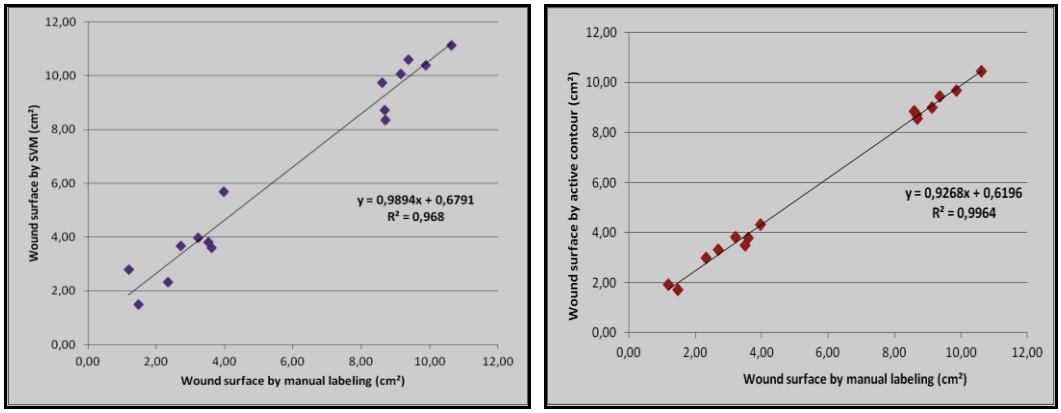

Figure 6. Comparison of methods: (left) the results of the SVM classification with R^2=0.96 and (right) the results of the active contour method with R^2=0.99.

The performance of the two methods was evaluated using sensitivity (Se) and specificity (Sp) measurements that were derived from the confusion matrix (Fig. 7 left). Other measurements namely the accuracy (P) and the success rate (T) were calculated using equations in figure 7 center. Results are illustrated in the table of the figure 7 right. It shows that there is a good equivalence between the two methods. The sensitivity and specificity values confirm that both methods have a good rate to detect regions considered as "wound" and to eliminate the class of "no wound". We note that the results obtained for the active contour method were calculated for all the database images. However, those obtained by SVM classification were computed on only half of the original database as this method needs a training step. Hence, for a single class approach, the active contour method presents a simple and good alternative for the SVM classification, proven effective in a multi-class in previous work[7], however it presents higher computational cost and rejects some aberrant results.

predict Class \ *True Class*	p	n
Y	True Positive	False Positive
N	False Negative	True Negative

$$Se = \frac{TP}{TP + FN}$$
$$Sp = \frac{TN}{TN + FP}$$
$$T = \frac{Se + Sp}{2}$$
$$P = \frac{TP + TN}{TP + FN + FP + TN}$$

SVM - AC	
Se	0,95
Sp	0,99
T	0,97
P	0,98

Figure 7. The confusion matrix (left), metrics equations (center), performances of the active contour method compared with the SVM classification (right).

3.3 Experimental results of multispectral images

The first processing performed to the multispectral images was the active contour method applied to the images acquired at 500 nm where we noted the highest disparities between the spectral signatures of the three tissue types of the wound. Fig. 8 shows an example of the obtained results. The active contour surrounded the homogenous region (granulation +

epithelium) of the wound. Fig 9 illustrates the results obtained after KNN classification applied in the multispectral images. We noted that three wound types were roughly distinguished: the healthy skin, the epithelium and the granulation. However, some errors were detected due to the reflection. Knowing the spatial resolution of the multispectral imaging system (*32 pixels.mm*$^{-1}$), the wound surfaces were calculated.

From the results previously described, we concluded that the active contour method could not distinguish between different tissues in the wound where the outline surrounded both the granulation and the epithelium without differentiation them. Figure 10 shows that the wound surfaces calculated by this method are higher than those calculated by the KNN classification that presented a better separation of tissue regions. The gap illustrated between the histograms represents the epithelium region that is not detected by the method of the active contour. Also, we concluded that wounds treated by pharmaceuticals (wounds 4 and 5), are not properly healed because of the small difference between the two histograms of the two methods.

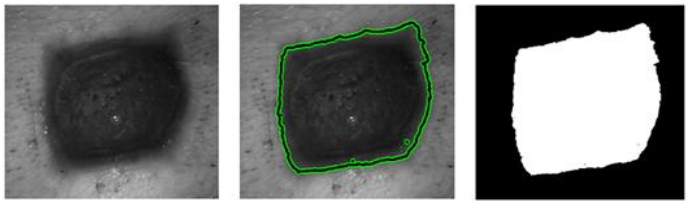

Figure 8. Result of the active contour method in a multispectral image at 500 nm: (a) original wound image, (b) the active contour surrounding the wound, (c) mask of the wound surface.

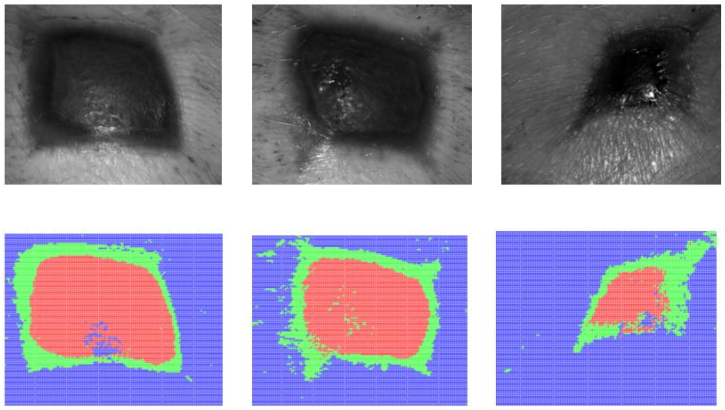

Figure 9. Results of the KNN classification in multispectral images with the detection of three wound types: (blue) healthy skin, (red) granulation and (green) epithelium.

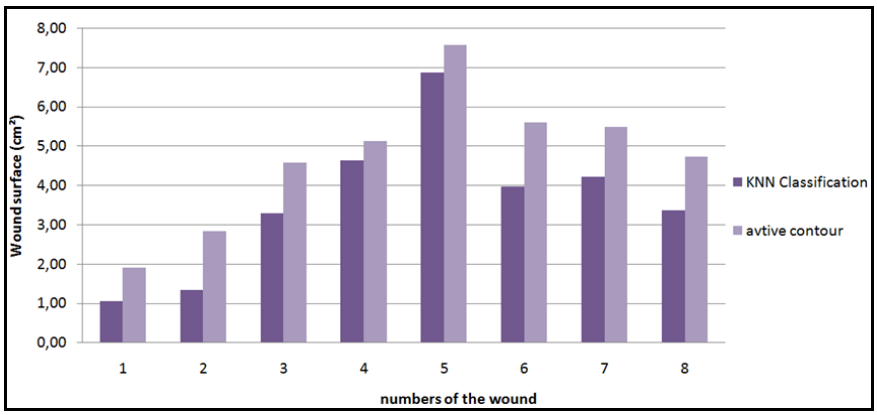

Figure 10. Comparison of the 8 wound surfaces calculated with two methods: (bright) active contour method, (dark) KNN classification method.

3.4 Comparison of wounds

During this study in apitherapy, the level of wounds healing had been evaluated. After calculating the wound surfaces in cm² (Table 1), they were standardized in percentage in order to compare the temporal wound healing evolution (Fig. 11). The rate of wounds healing was calculated for 5 sessions of images acquisition taken every 3 days during the study period. Table 2 and Figure 11 show that wounds treated with honey have a better healing level (wounds 2, 3, 6, 7) compared to wounds treated with pharmaceuticals. Thus, it proves that the medical thyme honey is a good natural product for healing wounds that could substitute conventional pharmaceuticals which are much more expensive.

Table 1. Measurements of wound surfaces *(cm²)* during 5 sessions of the study. The wounds 2, 3, 6, 7 were treated by medical thyme honey. The wounds 1, 4, 5, 8 were treated by pharmaceuticals.

	Wound 1	Wound 2	Wound 3	Wound 4	Wound 5	Wound 6	Wound 7	Wound 8
Session 1	7,62	9,35	8,85	8,68	8,91	8,08	7,91	7,41
Session 2	9,00	10,43	9,80	10,53	11,24	10,47	9,68	9,45
Session 3	4,10	5,94	7,60	7,95	8,68	8,06	8,54	8,31
Session 4	1,90	2,65	3,77	4,31	6,56	3,48	4,72	4,24
Session 5	1,38	1,72	3,31	3,58	5,43	3,81	3,47	2,97

Table 2. Level of wound healing *(%)*. The wounds 2, 3, 6, 7 were treated by medical thyme honey. The wounds 1, 4, 5, 8 were treated by pharmaceuticals.

	Wound 1	Wound 2	Wound 3	Wound 4	Wound 5	Wound 6	Wound 7	Wound 8
Session 1	0	0	0	0	0	0	0	0
Session 2	-1,4	-1,1	-1,0	-1,8	-2,3	-2,4	-1,8	-2,0
Session 3	3,5	3,4	1,2	0,7	0,2	0,0	-0,6	-0,9
Session 4	5,7	6,7	5,1	4,4	2,4	4,6	3,2	3,2
Session 5	6,2	7,6	5,5	5,1	3,5	4,3	4,4	4,4

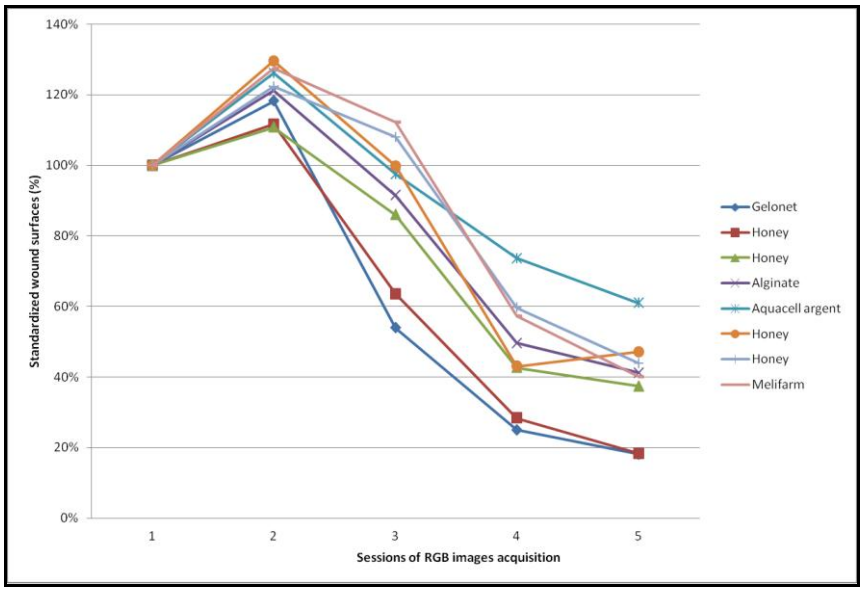

Figure 11. Standardized wound surfaces evolution during the study. Wounds treated with medical honey and Gelonet have the smallest surfaces. However, the most elevated surface is determined for the wound treated with Aquacel argent.

4. CONCLUSION

A comparative preclinical study was conducted in the context of apitherapy where RGB and multispectral images were processed in order to analyse wound healing evolution. Experimental results show that, for artificial wounds, active contour method is more efficient compared with supervised method such as SVM with tedious labelling and learning steps. Furthermore, we noted that multispectral imaging enables a deeper analysis of wound images where epithelial tissue can be clearly discriminated from granulation tissue, which is not the case with RGB imaging. In medical field, this study demonstrated that medical thyme honey is a relevant low cost alternative to commercial wound care products. Further experiments will be planned on three pigs with a new version of the prototype in order to validate the reproducibility of the experimental results and to enable full matching between colour and multispectral data.

ACKNOWLEDGMENTS

The authors would like to thank the French Conseil Régional Centre, and Ministère de l'Industrie, the European fund for regional development (FEDER) and the French OSéO for their financial support through the smart electricity cluster S2E2. The authors also thank the CHU of Limoges (Pr. Desmoulière and his team) for participation in this preclinical study.

REFERENCES

[1] Herbin, M., Bon, F. X., Venot, A., Jeanlouis, F., Dubertret, M. L., Dubertret, L. and Strauch, G., "Assessment of healing kinetics through true color image processing, " IEEE Transactions on Medical Imaging, 12(1), 39–43, (1993).
[2] Perez, A., Gonzaga, A. and Alves, J., "Segmentation and analysis of leg ulcers color images," in Proc. Int. Workshop on medical imaging and augmented reality, pp. 262–266, 10–12 June (2001).
[3] Oduncu, H., Hoppe, A., Clark, M., Williams, R. J. and Harding, K. G., "Analysis of skin wound images using digital color image processing: a preliminary communication," Int J Low Extrem Wounds, vol. 3, no. 3, pp. 151–156, Sep (2004).
[4] Belem, B., "Non-Invasive Wound Assessment by Image Analysis," PhD thesis, University of Glamorgan, Wales – UK (2004).
[5] Plassmann, P. and Jones, T., "Mavis: a non-invasive instrument to measure area and volume of wounds, " Medical Engineering and Physics, 20, 332–338, July (1998).
[6] Wannous, H., Lucas, Y., Treuillet, S., "Robust tissue classification for reproducible wound assessment in telemedicine environments," Journal of Electronic Imaging 19, 023002, Apr 08 (2010).
[7] Wannous, H., Lucas, Y., Treuillet, S., "Enhanced assessment of the wound-healing process by accurate multi-view tissue classification," IEEE Transactions on Medical Imaging, 30(2), pp. 315-326, February (2011).
[8] Masood, K., Rajpoot, N.M., Qureshi, H. and Rajpoot, K., "Hyperspectral Texture Analysis for Colon Tissue Biopsy Classification," International Symposium on Health Informatics and Bioinformatics, Antalya, Turkey, (2007).
[9] Qi, X., Xing, F., Foran, D. J. and Yang, L., "Comparative performance analysis of stained histopathology specimens using RGB and multispectral imaging," Proc. SPIE 7963, 79633B (2011).
[10] Jolivot, R., P. Vabres and Marzani. F., "An open system to generate hyperspectral cubes for skin optical refectance analysis," Skin Research and Technology, 16 (4), November (2010).
[11] De Roode, R., Noordmans, H. J., Verdaasdonk, R. and Sigurdsson, V., "Multispectral detectors: Multispectral system evaluates treatments in dermatology, " Laser Focus World, 42 (2006).
[12] Tomatis, S., Carrara, M., Bono, A., Bartoli, C., Lualdi, M., Tragni, G., Colombo, A., and Marchesini, R., "Automated melanoma detection with a novel multispectral imaging system: results of a prospective study, " Physics in medicine and biology, 50(8), 1675-1687(2005).
[13] Jakovels, D., Spigulis, J., Saknite, I., "Multi-spectral Mapping of In-vivo Skin Hemoglobin and Melanin," Progress in Biomedical Optics and Imaging, 11 (41), (2010).
[14] Yudovsky, D., Nouvong, A., Pilon, L., "Hyperspectral imaging in diabetic foot wound care," Journal of Diabetes Science and Technology, Volume 4, Issue 5, September (2010).
[15] Basiri, A., Nabili, M., Mathews, S., Libin A., Groah, S., Noordmans, HJ., Ramella-Roman, JC., "Use of a multi-spectral camera in the characterization of skin wounds," Optics Express,15, 18(4), 3244-57 (2010).

[16] Deng, Y. and Manjunath, B.S., "Unsupervised segmentation of color textures regions in images and video," IEEE Trans. on PAMI, vol. 23, no. 8, 140-147 (2001).
[17] Land, E. H., "The retinex theory of color vision," Scientific American, 108–128 (1977).
[18] Wannous, H., Treuillet, S. Lucas, Y., Mansouri, A. and Voisin, Y., "Design of a Customized Pattern for Improving Color Constancy Across Camera and Illumination Changes," in Proc. VISAPP (1), pp.60-67 (2010).
[19] Haralick, R. M., "Determining camera parameters from the perspective projection of a rectangle," Pattern Recognition, Volume 22, Issue 3, Pages 225-230 (1989).
[20] Kass, M., Witkin, A. and Terzopoulos, D., "Snakes: Active Contours Models, "Proceedings of the First International Conference on Computer Vision, pp.259-268, (1987).
[21] Li, C., Liu, J. and Fox, M. D., "Segmentation of external force field for automatic initialization and splitting of snakes," Pattern Recognition, vol.38 (11), pp.1947–1960 (2005).
[22] Lankton, S. and Tannenbaum, A., "Localizing Region-Based Active Contours," IEEE Transactions on Image Processing 17(11), 2029-2039 (2008).
[23] Mumford, D. and Shah, J., "Optimal approximation by piecewise smooth functions and associated variational problems," Commun. Pure Appl.Math, vol. 42, pp. 577–685 (1989).
[24] Osher, S. and Sethian, J. A. "Fronts propagating with curvature-dependent speed: Algorithms based on Hamilton–Jacobi Formulation, " J. Comput. Phys., vol. 79, pp. 12–49 (1988).
[25] Chan, T. and Vese, L., "Active Contours Without Edges", IEEE Transactions on Image Processing, vol10(2), 266-277(2001).
[26] Lankton, S. Active Contour Segmentation, (Updated 15 Apr 2008)
http://www.mathworks.com/matlabcentral/fileexchange/19567
[27] Jolivot, R., Nugroho, H., Vabres, P., Fadzil, M.H.A. and Marzani. F., "Validation of a 2D multispectral camera: application to dermatology/cosmetology on a population covering five skin phototypes, " Proceedings of SPIE, 8087, 808729 (2011).
[28] Jolivot, R., Vabres, P., and Marzani, F., "Reconstruction of hyperspectral cutaneous data from an artificial neural network-based multispectral imaging system, "Computerized medical imaging and graphics, 35, 85-88 (2010).
[29] Cooper, T. M. and Hart, P. E., "Nearest Neighbor Pattern Classification," IEEE Transactions on Information Theory, IT-13 21-27, (1967).
[30] Larson, S., "The shrinkage of the coefficient of multiple correlation," J. Educat. Psychol., 22, 45–55, (1931).
[31] Célisse, A., Mary-Huard, T., "Exact Cross-Validation for kNN and applications to passive and active learning in classification," Journal de la Société Française de Statistique, vol. 152, iss. 3, (2011).